Int. J. Electrochem. Sci., 7 **(2012)** 1242 - 1250

International Journal of
ELECTROCHEMICAL
SCIENCE
www.electrochemsci.org

Anisotropic Expansion and High Rate Discharge Performance of V-doped MnO_2 for Li/MnO_2 Primary Battery

Shengping Wang[1,*], *Qiuling Liu*[1], *Jingxian Yu*[2], *Jian Zeng*[1]

[1] Faculty of Material Science and Chemical Engineering, China University of Geosciences, Wuhan 430074, PR China
[2] School of Chemistry and Physics, The University of Adelaide, Adelaide, SA 5005, Australia
[*]E-mail: robert@cug.edu.cn

Received: 12 December 2011 / *Accepted:* 13 January 2012 / *Published:* 1 February 2012

V-doped MnO_2 (VHEMD) has been prepared by thermally treating the mixture of electrolyzed manganese dioxide (EMD) and V_2O_5 powder and characterized using cyclic voltammetry (CV), constant current discharge, electrochemical impedance spectroscopy (EIS) and X-ray diffraction technique. CV results showed that VHEMD has a much higher reduction peak current than that of only thermally treated electrolyzed manganese dioxide (HEMD), though both have a similar reduction potential. Constant current discharge measurements showed VHEMD exhibits an improved high rate discharge performance. VHEMD reaches a maximum discharge capacity of 202 mAh g^{-1} at a high rate (2 mA cm^{-2}), which is considerably higher than that of HEMD (155 mAh g^{-1}), although both HEMD and VHEMD have similar discharge capacity at a low rate (0.1 mA cm^{-2}). EIS results demonstrated that both Li^+ insertion resistance (R_{ct}) and Li^+ diffusion impedance (W) in VHEMD were always lower than those of HEMD at any depth of discharge (DOD). XRD results confirmed that V-doping leads to an anisotropic expansion of MnO_2 lattice, with *a* axis slightly elongated by 0.74% and *c* axis slightly shortened by 0.17%. The improved crystal structure after V-doping can be attributed to the faster kinetics of both Li^+ insertion and diffusion in VHEMD.

Keywords: Li/MnO_2 primary battery, electrolyzed manganese dioxide, V-doped, High rate discharge performance

1. INTRODUCTION

With the advantages of low cost, environmentally friendliness and high energy density, Li/MnO_2 primary battery, as one of the most important primary batteries, has been widely used in low power consumption applications, for example power supply for computer motherboards and accutrons. However the poor high rate discharge performance prevents their high power output applications, e.g. the military communicative devices and civil smart meters [1, 2]. It has been proved that both the

electrochemical reaction of Li and the conductivity of electrolyte are suitable for high rate discharge applications. Therefore MnO_2 cathodes are the limiting factor for high rate performance in Li/MnO_2 primary batteries. The conventional cathode active material in Li/MnO_2 primary batteries is thermally treated electrolyzed manganese dioxide (HEMD), which is a mixture of pyrolusite-MnO_2 (*p*-MnO_2, 65-85 wt%) and ramsdellite-MnO_2 (*r*-MnO_2) [3, 4]. Under a low power output condition (25 ^oC, 0.1 mA cm^{-2}), the discharge capacity of HEMD can reach 90% for the theoretical capacity of MnO_2. However, at a high discharge rate, i.e. 25 ^oC and 2 mA cm^{-2}, the discharge capacity remarkably decreases to only 55% of the theoretical capacity. In past decades, a large amount of efforts have been attempted to improve the high rate discharge performance of MnO_2 cathodes. An improved high rate discharge performance can be achieved by reducing the electrode thickness [5, 6] and improving the porosity [5] through cathode structural modification. However the energy density of battery is sacrificed to some extent. Additionally, conductive additives (such as Ag [7], carbon [8, 9]), or preprocessing MnO_2 in O_2/Air atmosphere [10, 11, 12], only show very limited improvements.

Regarding the discharge process in Li/MnO_2 batteries, Li^+ ions first insert into MnO_2 lattice across the MnO_2/electrolyte interface and then diffuse within MnO_2 lattice to produce Li_xMnO_2 (x=0~1) complexes. Apparently, HEMD can satisfy a moderate insertion and diffusion velocity at a low discharge rate. However the nature of slow Li^+ ions insertion and diffusion kinetics within MnO_2 lattice restricts high rate discharge performance of MnO_2 cathodes due to the high electrochemical polarization caused by a high rate discharge current density. Since the slow Li^+ ions insertion/diffusion kinetics in HEMD cathode is the determining factor that confines the high rate electrochemical performance, ameliorating the lattice feature of MnO_2 in HEMD to facilitate Li^+ ions insertion and diffusion properties could be an effective method to improve the high rate performance of Li/MnO_2 batteries. It has already been reported that, doping vanadium into spinal $LiMn_2O_4$ materials can improve the electrochemical performance of rechargeable $LiMn_2O_4$ batteries [13]. Therefore one could expect that V-doping could also affect the HEMD lattice parameters and hence achieve better Li^+ ions insertion and diffusion kinetics.

In this paper, we attempted to synthesize V-doped HEMD (VHEMD) by thermally treating the mixture of V_2O_5 and electrolyzed manganese dioxide (EMD, MnO_2 content of EMD sample is 91%). Indeed, VHEMD exhibits a remarkably improved high rate discharge capacity in comparison with conventional HEMD.

2. EXPERIMENTAL

The mixture of EMD (Xiangtan, China, 98 wt%) and V_2O_5 (AR, 2 wt%) was first mechanical ball milled for 20 minutes and then thermally treated at 375 ^oC for 10 h in an air flow to yield VHEMD. The Mn:V ratio within VHEMD was identified to be 50:1 using ICP-MS (Thermo Electron X7 ICP-MS, USA) element analysis. HEMD was prepared by processing only EMD through exactly the same procedure. VHEMD or HEMD was then mixed entirely with graphite and acetylene black at a weight ratio of 85:7.5:7.5. Then 1.762 g of resulting mixture (either VHEMD or HEMD mixture) was stirred in 100 g of polyvinylidene fluoride (5 wt%) / N-methyl pyrrolidone solution for 10 minutes

to generate a slurry. The slurry was coated onto a thin aluminum foil with a thickness of 0.15 μm. After dried at 105 ^{o}C under vacuum for 12 h, they were chopped into either square or round-shaped electrodes. Before any electrochemical measurements, all of these electrodes were further dried at 200 ^{o}C under vacuum for 12 h. Round-shaped electrodes with a diameter of 15 mm and a thickness of 60 μm were assembled into test cells (2025) using a lithium negative electrode and a Cegard2400 separator. Square electrodes, with an area of with 0.04 mm^2, were employed as a working electrode in a three-electrode system with lithium foil as both the reference electrode and counter electrode. Both test cells and three-electrode systems were assembled in Ar atmosphere using 1 M $LiClO_4$: PC: DME (volume ratio of PC to DME is 1:1) as electrolyte.

Constant current discharge measurements were performed on a RT-F Battery Analyser (Luhua, China) with a current density of 0.1 or 2 mA cm^{-2} at 25 ^{o}C respectively. The cut-off voltage was set to be 2.0 V. Both cyclic voltammetry (CV) and electrochemical impedance spectroscopy (EIS) were performed on a CHI660C electrochemical workstation (CHI, China).The CV was carried out in a potential range of 3.2-1.0 V with scan rates of 0.05, 0.25, 0.50 and 1.00mV s^{-1} respectively. The amplitude of the AC signal for EIS was set at 5 mV and the frequency was ranged from 10^{-2} to 10^5 Hz. A X'pert PRO DY2198 X-ray powder diffractometer (PANalytical, Netherlands) was employed to characterize the crystal structures of HEMD and VHEMD (Cu Kα radiation, 10°-90°).

3. RESULTS AND DISCUSSION

Fig. 1 shows the CV curves of HEMD and VHEMD at different scan rates. The reduction peak potential of VHEMD appears around 2.3 V at a fast scan rate (1 mV s^{-1}) and shifts to an anodic direction with the decrease of scan rate, around 2.57 V at a scan rate of 0.05 mV s^{-1}. The CV feature of HEMD shows some similarity to that of VHEMD with the reduction peaks positioning in the range of 2.3-2.6 V. Both HEMD and VHEMD exhibit only one reduction peak without any oxidation peak in our experimental scope, which is in consistent with the typical single electron reduction mechanism of MnO_2 [14]. It can thus be concluded that the V-doping does not change the electrochemical reaction mechanism in MnO_2 cathode materials. However the reduction peak current of VHEMD is obviously higher than that of HEMD at the same scan rate, indicating that the diffusion and insertion of Li^+ ions is remarkably improved in VHEMD. Based on their CV data, the apparent electron transfer rate constants k_0 [15] in both VHEMD and HEMD are estimated.

$$I_p = 0.227nFAC_0k^0e^{[-\frac{\alpha F}{RT}(E_p - E^{0'})]}$$

Where I_p is the peak current of the cathodic MnO_2 reaction, E_p is the peak potential, n is the electrons in the reaction, A is the area of the electrode, C_0 is the initial concentration of reactants, α is the transfer coefficient, $E^{0'}$ is the apparent potential of electrode. The k_0 of VHEMD (3.82×10^{-12} cm s^{-1}) is 1.7 times greater than that of HEMD (2.25×10^{-12} cm s^{-1}), suggesting that the V-doping improves

the tunnel structures in MnO_2 and consequently facilitates the electrochemical reduction process of MnO_2. Thus an improved high rate discharge property can be expected in VHEMD in comparison with conventional HEMD.

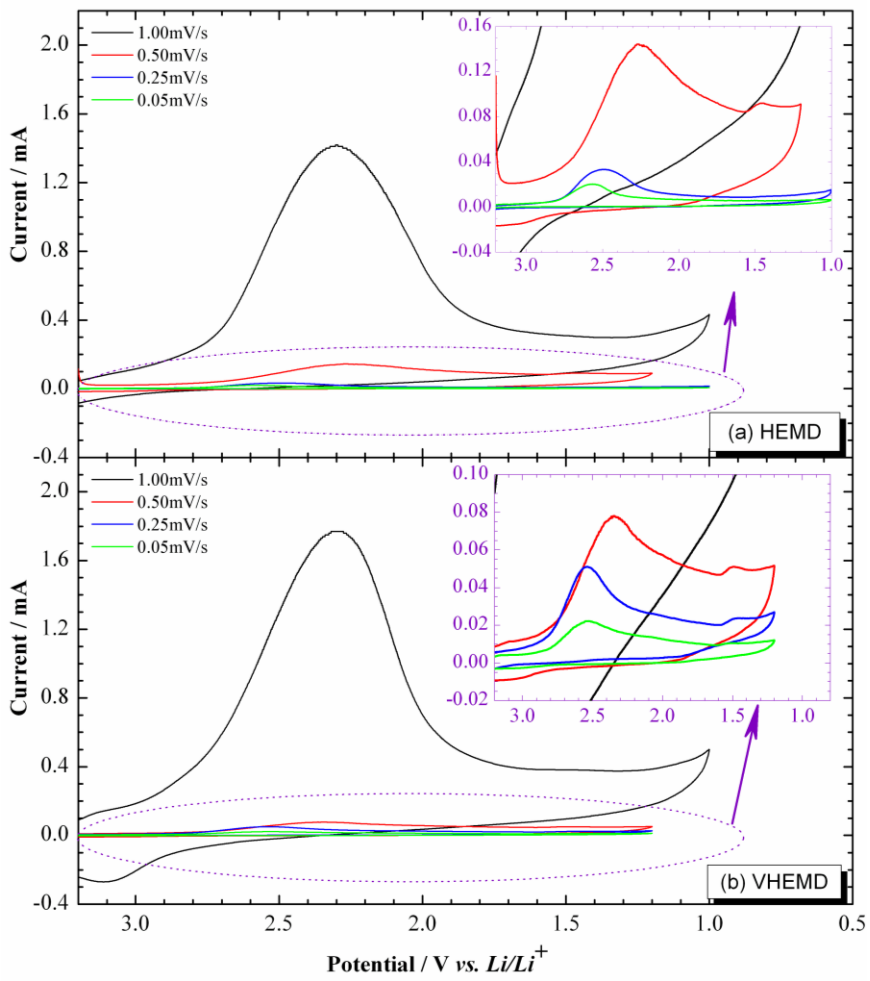

Figure 1. The cyclic voltammetric curves of (a) HEMD and (b) VHEMD.

Constant current discharge measurements were conducted within HEMD and VHEMD test cells. Their constant current discharge curves were shown in Fig. 2. The available discharge capacity in both HEMD and VHEMD reaches 258 mAh g^{-1} (92% theoretical capacity of MnO_2) at a low rate discharge current density of 0.1 mA cm^{-2} with a cut-off voltage of 2.0 V. The only difference is that the discharge plateau of VHEMD is slightly higher than that of HEMD. At a high rate discharge current density (2 mA cm^{-2}), VHEMD shows a much higher discharge voltage plateau (2.6 V of VHEMD vs. 2.2 V of HEMD). More importantly, the available capacity of VHEMD attains 202 mAh g^{-1} (72% of the theoretical capacity), which is considerably higher than that of HEMD (155 mAh g^{-1}).

Fig. 3 depicts the EIS spectra of both HEMD and VHEMD with different depth of discharge (DOD). These EIS spectra exhibit a typical feature of Li^+ ions insertion to MnO_2 lattice in the high frequency region and Li^+ ions diffusion within MnO_2 lattice to form nonstoichiometric Li_xMnO_2 (x=0~1) complexes in the low frequency region. Using the equivalent circuit model (as shown in Fig.

4) proposed by Aurbach et al [16], we obtained the Li^+ ions insertion resistance (R_{ct}) through the liquid-solid interface as shown in Fig. 5(a).

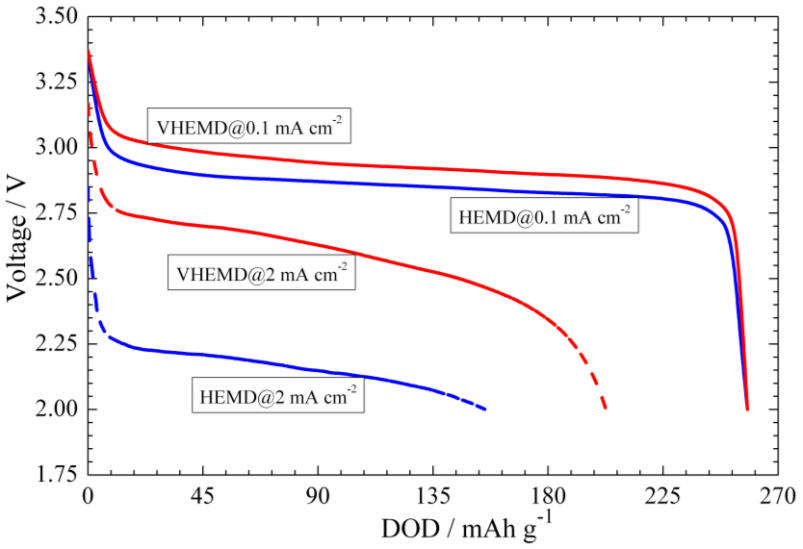

Figure 2. The discharge curve of HEMD and VHEMD.

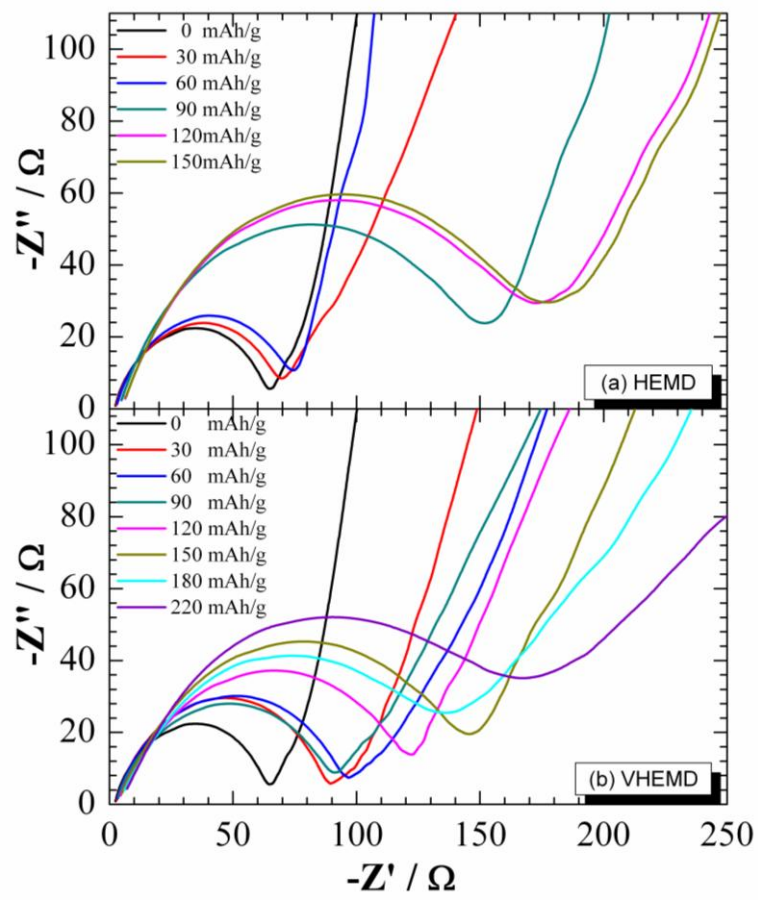

Figure 3. EIS spectra of both (a) HEMD and (b) VHEMD at different DODs.

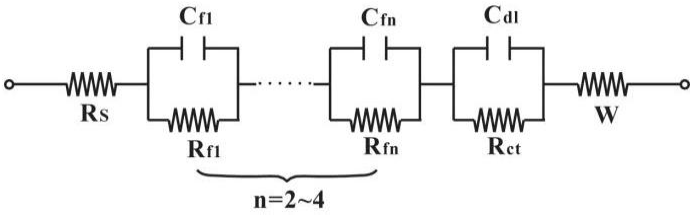

Figure 4. The equivalent circuit model for the EIS spectra of both HEMD and VHEMD. Where R_s is the electrolyte resistance, the impedance of capacitance $C_{fn(n=2\sim4)}$ and impedance $R_{fn(n=2\sim4)}$ in parallel is the electrode surface film resistance, C_{dl} is the double-layer capacitance of the material interface, R_{ct} is the charge transfer resistance, W is the diffusion resistance of the Li^+ ions within the MnO_2 lattice.

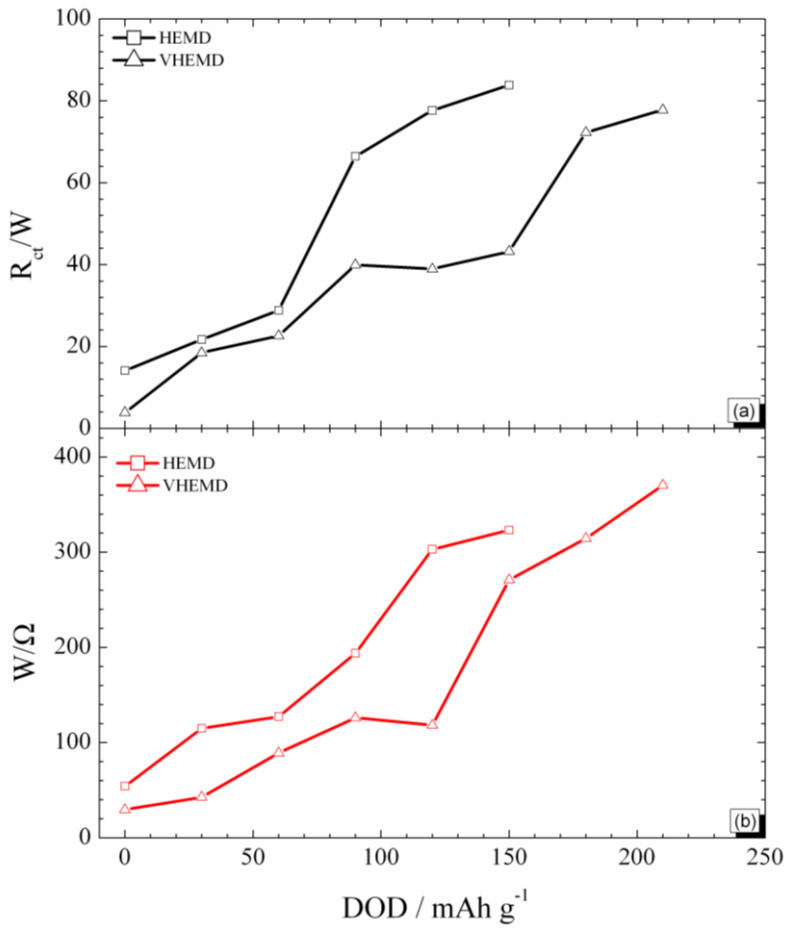

Figure 5. Plots of (a) Li^+ ions insertion impedance (R_{ct}) and (b) Li^+ ions diffusion impedance (W) vs. depth of discharge.

The R_{ct} of initial VHEMD cathode is 3.88 Ω (DOD=0), which is remarkably lower than that of HEMD (14.14 Ω). As more and more Li^+ ions insert into the lattice, the R_{ct} in both HEMD and VHEMD increases simultaneously while the R_{ct} values in VHEMD are always lower than those of HEMD, implying that VHEMD is capable of providing faster Li^+ ions insertion kinetics than HEMD at any DOD. Also we observed that the Li^+ ions diffusion impedance (W) of VHEMD at any DOD is

lower than that of HEMD as shown in Fig. 5(b). Low Warburg impedance means that VHEMD enables a faster Li^+ ions diffusion process within lattice, which could be the reason why VHEMD reduces the electrochemical polarization and hence exhibit better high rate discharge performance.

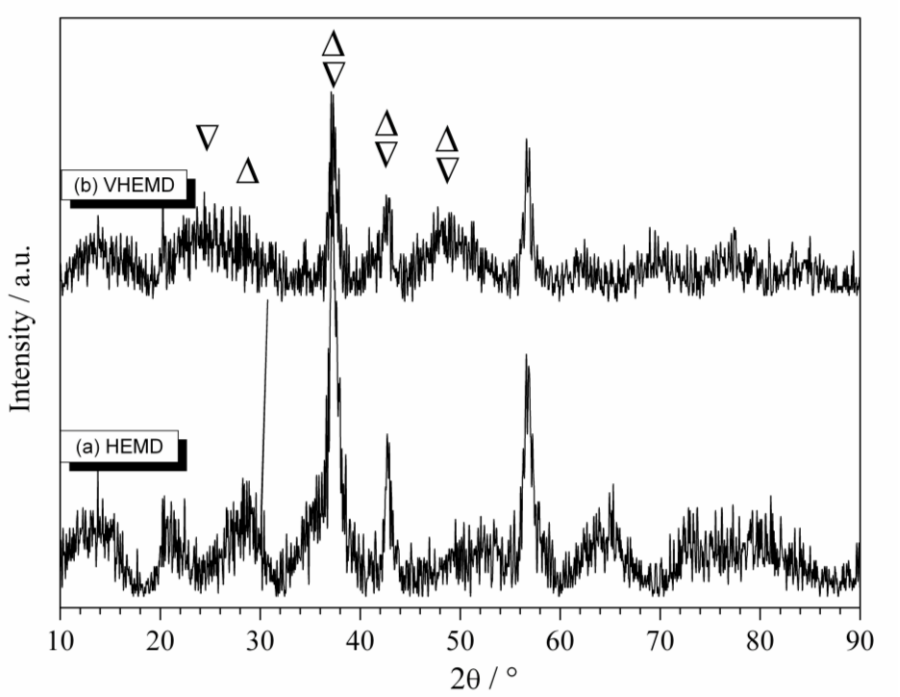

Figure 6. XRD patterns of (a) HEMD and (b) VHEMD powders, where △ represents pyrolusite and ▽ represents ramsdellite phases.

In order to understand the structural difference in HEMD and VHEMD, the XRD patterns of both powders are characterized as shown in Fig. 6. Strong peaks of *p*-MnO_2 are observed at similar positions in both VHEMD and HEMD, while none of the V_2O_5 feature appears in Fig. 6(b). It can be concluded that, through the thermal treatment at 375 ^oC, V_2O_5 has incorporated into MnO_2 lattice forming a new $Mn_xV_{1-x}O_2$ (x=0~1) binary oxide phase [17, 18]. The calculated lattice parameters for most *p*-MnO_2 are listed in Table 1.

Table 1. The calculated lattice parameters for *p*-MnO_2 of HEMD and VHEMD.

	***a*(Å)**	***c*(Å)**	***v*(Å^3)**
HEMD	4.3792	2.9021	55.6546
VHEMD	4.4115	2.8971	56.3808

Upon the doping of V, an anisotropic expansion for MnO_2 lattice occurs. The *a* axis is slightly elongated by 0.74% while the *c* axis is slightly shortened by 0.17%. The unit cell volume expansion is

calculated to be 1.30%. Since Li^+ ions insert through the (001) face and diffuse through [1×1] tunnels along *c*-axis of *p*-MnO_2 [14], apparently a large *a* axis enables the interfacial Li^+ insertion easier, and also a smaller *c* axis facilitates Li^+ diffusion from the outer sites to inner sites within the lattice of *p*-MnO_2.

4. CONCLUSIONS

We synthesized V-doped MnO_2 as cathode materials for Li/MnO_2 primary battery. Due to the anisotropic expansion of MnO_2 lattice by introducing vanadium, [1×1] tunnels are expanded and also the *c* axis is shortened. Consequently this anisotropic expansion leads to a favorable electrochemical process for Li^+ ions insertion and diffusion, allowing fast reduction kinetics of MnO_2. The discharge capacity of VHEMD is significantly improved to 202 mAh g^{-1} at the high rate discharge current density of 2 mA cm^{-1} with a cut-off voltage of 2.0 V, compared to 155 mAh g^{-1} of HEMD at the same condition. By optimizing the doping rate or using different doping elements, we can further make the high-rate performance reach the maximal capacity for MnO_2 based Li/MnO_2 primary batteries. We will report the corresponding results in extended papers in the near future.

ACKNOWLEDGEMENTS
This work was financially supported by the National Natural Science Foundation of China (21173198) and the Natural Science Foundation of Hubei Province, China (2008CDB018).

References

1. M.S. Park and W.Y. Yoon, *J. Power Sources*, 114 (2003) 237-243.
2. Y.Y. Yang, L.F. Xiao, Y.Q. Zhao and F.Y. Wang, *Int. J. Electrochem. Sci.*, 3 (2008) 67-74.
3. S. Jouanneau, S. Sarciaux, A. Le Gal La Salle and D Guyomard, *Electrochim. Acta*, 48 (2002) 11-20.
4. A.Walker and T.F. Reise, *US Patent* 4921689 A (1990).
5. M. Okada and H. Yasuda, *US Patent* 6534218 B1 (2003).
6. M.Voinov, *Electrochim. Acta*, 27 (1982) 833-835.
7. Y. Yang, X.K. Huang and H.J. Yue, *CN Patent* 1688047 A (2005).
8. C.A. Frysz, X.P. Shui and D.D.L. Chung, *J. Power Sources*, 58 (1996) 41-54.
9. Y. Yang, X.K. Huang and H.J. Yue, *CN Patent* 1750298 A (2006).
10. K.S. Lyons and D.R. Rolison, *US Patent* 7618609 B2 (2009).
11. S. Hiroshi, N. Yoshio and D. Takuya, *JP Patent* 07-272716 (1995).
12. F.J. Kruger, *US Patent* 4405699 (1983).
13. A.Eftekhari, *Solid State Commun.*, 140 (2006) 391-394.
14. T. Ohzuku, M. Kitagawa and T. Hirai, *J. Electrochem. Soc.*, 136 (1989) 3169-3174.
15. A.J. Bard and L.R. Faulkner, *Electrochemical Methods, Fundamentals and Applications*, John Wiley & Sons, New York, USA (1980).

16. D. Aurbach, B. Markovsky, M.D. Levi, E. Levi, A. Schechter, M. Moshkovich and Y. Cohen, *J. Power Sources*, 81-82 (1999) 95-111.
17. N. Kumagai, S. Tanifyji and K. Tanno, *J. Power Sources*, 35 (1991) 313-322.
18. F. Rubio-Marcos, A. Quesada, M.A. García, M.A. Bañares, J.L. G.Fierro, M.S.Martín-Gonzalez, J.L. Costa-Krämer and J.F. Fernández, *J. Solid State Chem.*, 182 (2009) 1211-1216.